
Title: Mass Transport Limitations in Microbial Fuel Cells: Impact of Flow Configurations

Authors: Thomas Krieg, Jeffery A. Wood, Klaus-Michael Mangold, Dirk Holtmann

PII: S1369-703X(18)30275-4
DOI: https://doi.org/10.1016/j.bej.2018.07.017
Reference: BEJ 7003

To appear in: *Biochemical Engineering Journal*

Received date: 31-3-2018
Revised date: 5-6-2018
Accepted date: 17-7-2018

Please cite this article as: Krieg T, Wood JA, Mangold K-Michael, Holtmann D, Mass Transport Limitations in Microbial Fuel Cells: Impact of Flow Configurations, *Biochemical Engineering Journal* (2018), https://doi.org/10.1016/j.bej.2018.07.017

# Mass Transport Limitations in Microbial Fuel Cells: Impact of Flow Configurations

Thomas Krieg[1], Jeffery A. Wood[2], Klaus-Michael Mangold[3], Dirk Holtmann[1]*

*corresponding author

Email: holtmann@dechema.de

**Affiliations**

[1]Industrial Biotechnology, DECHEMA Forschungsinstitut, Theodor-Heuss-Allee 25, 60486 Frankfurt am Main, Germany

[2]Soft Matter, Fluidics and Interfaces, Faculty of Science and Technology, University of Twente, Drienerlolaan 5, 7522NB, Enschede, The Netherlands

[3]Electrochemistry, DECHEMA Forschungsinstitut, Theodor-Heuss-Allee 25, 60486 Frankfurt am Main, Germany

## Highlights

- Perpendicular flow through the anode increases MFC performance by a factor of 3.2
- Biofilm growth is increased by perpendicular flow through the anode
- Simulations show an improved substrate distribution for the perpendicular flow

## Abstract

The performance of microbial fuel cells (MFCs) is limited by a number of factors, including metabolic activity of electroactive microorganisms and electrochemical systematic constraints, such as

overpotentials at the electrodes or IR losses. Heterogeneities of substrate distribution (availability) can also strongly limit current in MFCs. In this work we investigate how mass transport can be enhanced by changing the flow configurations in MFCs, e.g. by directing the flow through a porous anode or by applying inserts and channels to anodes. Experimental results using a perpendicular flow through the anode were compared to a parallel flow setup, showing increased current output. Finite element method (FEM) simulations were used to simulate the flow profiles and substrate distribution in each setup. The simulations revealed higher average substrate concentrations for the perpendicular flow through a porous carbon fabric anode *vs.* a parallel flow in the bulk phase of the MFC, related to the enhancement of transport via convection in perpendicular flow. The simulated substrate distributions found for the different inlet setups could be correlated to the experimentally obtained current flow, power output and biofilm distribution. It can be concluded that the increased current output can be explained by the flow profile in the system resulting in an increased substrate distribution in the biofilm on the electrode and a hindered oxygen transport from the cathode.

**Abbreviations:**CE: Coulombic efficiency

- CFD: Computational fluid dynamics
- DAPI: 4',6-diamidino-2-phenylindole
- FEM: Finite element method
- MFC: Microbial fuel cell

**Keywords:** Computational fluid dynamics; microbial fuel cells; *Geobacter sulfurreducens*; heterogeneities; substrate distribution; bioelectrochemical system

## 1. Introduction

Microbial fuel cells (MFCs), as well as microbial electrolysis cells (MECs), have a great impact in the area of renewable power generation. The MFCs have the advantage in generating power from waste compared to anaerobic digestion, as the electrical energy harvested by MFCs is considered as a "cleaner" energy compared to the $CH_4$ or $H_2$ produced by anaerobic digestion [1]. Organic loadings of waste streams can be broken down by electroactive bacteria to carbon dioxide and electrons, which are transferred to an electrode, clearing wastewater [2–4]. In recent decades success has been achieved scaling-up MFCs to the level of pilot plants, however only one commercial MFC is known to date [5–7]. Many sophisticated technical designs to prevent mass transport limitations have been investigated in several reactor types using simulations and comparison to experimental data [8–10]. Flat plate reactors have been used for a scale-up of a microbial electrolysis cell leading to several key results, one of them suggesting special attention towards fluid dynamics in the anode chamber is required to prevent mass transport limitations [11]. These limitations can be overcome by system design, which can be a low cost method to overcome substrate limitations. Structuring the interior of anodes for a better mass transport, high retention times and low electrode spacing are beneficial for MFC performance [8,12,13]. When comparing different electrode materials, porous carbon based electrodes, such as carbon fabric, showed best results compared to electrode material such as carbon based foils, felts or paper [14]. This is due to a higher electroactive surface area accessible for the electroactive bacteria. Further improvement has been done by altering the flow configuration through porous electrodes [13,15]. Perpendicular flow through porous anodes of MFCs showed lower internal resistance and increased performance [13]. Further studies in MECs have been conducted and forcing the flow through the anode also increased the performance. The authors postulated that an increased mass transport in the anode leading to a more distributed substrate supply to the biofilm is responsible for the better performance [15]. Further explanations are that no oxygen is measured in front of the anode and the transport of protons away from the biofilm is enhanced if the flow is directed through the anode towards the cathode. This is an interesting hypothesis but requires further investigation and

is beyond the scope of this work. Before this more complicated hypothesis is considered, a more detailed understanding of the fluid transport phenomena in MFC systems needs to be investigated.

To date, less is known about the distribution of substrates in MFCs, particularly in porous electrodes, which may be key parameter of MFC performance [13,15,16]. To get more insight into the nature of transport limitations and performance in an MFC a cubic reactor was constructed and characterized experimentally, combined with numerical simulation of the flow patterns and distribution of substrate in the MFC. Two flow setups and their influence on substrate distribution in the bulk phase of the reactor and the porous anode itself were compared: i) parallel flow over a porous anode and ii) perpendicular flow through a porous anode. For further insight into the differences in performance for each configuration, simulations based on the finite element method were performed to obtain the flow profile based on the Navier-Stokes (fluid domain) and Brinkman equations (porous domain). Furthermore, the species distribution using an convection-diffusion equation, with the diffusion of species in the porous layer described by the Bruggeman relationship is simulated [17–19]. The results of these simulations were then used to help interpret the experimental results with regard to performance and biofilm distribution in the continuous MFC.

## 2. Materials and Methods

### 2.1 Design of an air-breathing microbial fuel cell

A reactor for the microbial fuel cell experiments was designed based on a flat-plate design using Solid Edge® (Siemens PLM Software, Plano, TX; USA). End plates of the reactor (outside measurements: width=100 mm, height=150 mm, depth=5 mm) and reaction chamber (outside measurements: width=100 mm, height=150 mm, depth=10 mm; inside measurements of the actual reaction chamber: width=60 mm, height=10 mm, depth=10 mm) were made of polyetheretherketone (PEEK) due to its chemical and mechanical stability. Electrodes were contacted using a graphite foil as a current collector (d=0.25 mm, #009077, MaTecK GmbH, Jülich, Germany), which was pressed onto the electrodes in between two silicon rubber foils (d=1 mm, Schulz & Souard, Frankfurt am Main, Germany) sealing the

reactor by the end plates to the reaction chamber and the end plates were fixed with screws and nuts. The end plate for the gas diffusion cathode was open to the air to allow oxygen to reach the catalyst. A scheme with the investigated flow setups is shown in Figure 1 and a picture of the used MFC is shown in Figure S1.

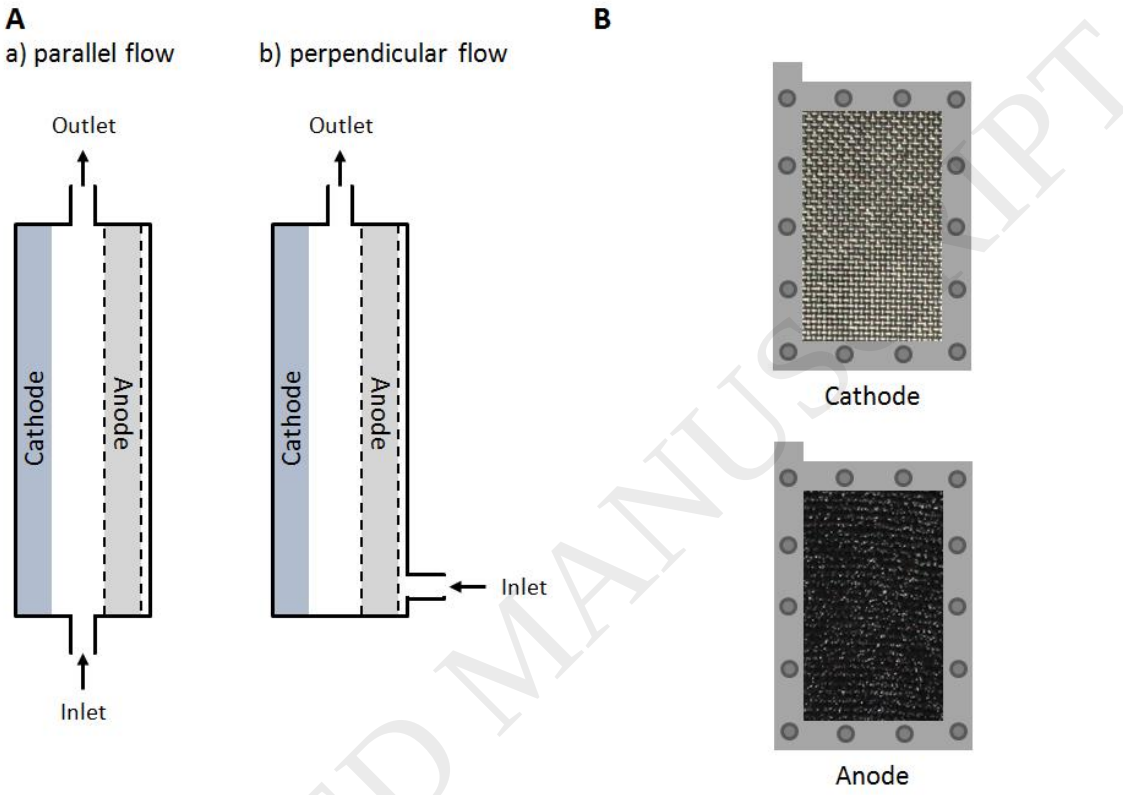


**Figure 1: Scheme of the designed air-breathing microbial fuel cell (A, side view) and the electrode-current collector assemblies of the air-breathing cathode and the porous anode (B).**

For perpendicular flow through the anode the corresponding end plate at the anode side was opened up by drilling to fit a hollow screw, which served as inlet (Figure 1). For a flow parallel over the anode the reactor chamber was opened up by drilling at the side to fit a hollow screw, which served as inlet in this case (Figure 1).

### 2.2 Characterization of the flow regime in microbial fuel cells with varied electrode setup and inlet

In order to understand the nature of the flow profiles for the different inlet configurations, models of each system were constructed in COMSOL Multiphysics® 5.2 (Boston, MA, USA). For each model, the

fluid flow and concentration profiles for substrate were simulated. To describe the fluid flow in the bulk (non-porous) environment the Navier-Stokes equations were solved (eq. 1 and 2) for the momentum balance (1) and continuity equation (2).

$$\rho(\vec{\mathbf{u}} \cdot \nabla\vec{u}) = -\nabla p + \mu\nabla^2\vec{u} \qquad (1)$$

$$\nabla \cdot \vec{\mathbf{u}} = 0 \qquad (2)$$

In (1) and (2), $\vec{u}$ is the velocity vector, $p$ the pressure, $\rho$ the fluid density and $\mu$ the fluid viscosity. For the porous domain, the flow profile was solved via the Brinkmann formulation (3) coupled to the continuity equation (2) [19].

$$\rho\left(\frac{\vec{\mathbf{u}}\cdot\nabla\vec{u}}{\boldsymbol{\varepsilon_p^2}}\right) = -\nabla p + \frac{\mu\nabla^2\vec{u}}{\varepsilon_p} - \left(\frac{\mu}{\kappa}\right)\vec{\mathbf{u}} \qquad (3)$$

In (3), $\varepsilon_p$ is the porosity and $\kappa$ is the permeability of the porous layer.

This velocity profile couples to the concentration profile of substrate in the system, which was determined in a transient fashion. This allowed for determining the effective concentration of substrate within the porous layer as a function of time/effectiveness of substrate distribution in the porous layer, for different porous layer properties (porosity and permeability). In the bulk, the concentration profile is solved as a transient convection-diffusion problem with diffusion governed by Fick's law (dilute conditions, eq. 4),

$$\frac{\partial c}{\partial t} + \nabla \cdot (-D\nabla c + \vec{u}c) = 0 \qquad (4)$$

where c is the concentration of substrate (acetate) and $D$ the substrate diffusion coefficient.

For the porous layer, the diffusion is modified by the tortuosity of the porous layer and this is treated by the Bruggeman relationship [17,18]. For the Bruggeman relationship, tortuosity ($\tau$) is given as $\tau = {1}/{\varepsilon_p^{1/2}}$ and the diffusion coefficient in the porous layer ($D_{pl}$) is then given as $D_{pl} = D\frac{\epsilon_p}{\tau}$ [17]. Dispersion and adsorption into the porous layer were neglected in this simple model, where the goal was purely

to determine the effect of changing the cloth permeability/porosity on the predicted flow profiles for the two MFC configurations. This then leads to the final equation 5.

$$\varepsilon_p \frac{\partial c}{\partial t} + \nabla \cdot \left(-D_{pl} \nabla c + \vec{u} c\right) = 0 \qquad (5)$$

For boundary conditions, the inlet was considered an inflow for fluid (under laminar conditions) and a constant concentration representing the inflow of substrate for the concentration profile. The outlet was considered a constant pressure condition for fluid (set at an arbitrary value of zero to specify the pressure within the domain) and an outflow condition for concentration (no-gradient). All other exterior boundaries were set as no-slip (zero wall velocity) and no-flux (impermeable walls).

The liquid density is assumed to be that of pure water, i.e., $\rho=10^3$ kg m$^{-3}$ with a viscosity of $\mu=10^{-3}$ Pa s. The properties of the carbon fabric anode (ACC-5092-15, Kynol, Hamburg, Germany) were provided by the supplier, the porosity was $\varepsilon_p=0.86$ and the permeability $\kappa=10^{-10}$ m². The equations were solved numerically using COMSOL Multiphysics® 5.2 with a relative tolerance of 0.001. P2+P1 discretization (second-order Lagrange elements for velocity and first-order elements for pressure) was used to solve the Navier-Stokes equations and first-order Lagrange elements for the concentration profile. The mesh was refined near the walls and independency was checked. The complete mesh consisted of approximately 600,000 domain elements. The distribution of the organic compound used as a substrate, acetate, was simulated with the equations listed above for a diffusion coefficient of approximately $0.9 \cdot 10^{-9}$ m² s$^{-1}$ for both perpendicular flow and parallel flow through the porous anode [20].

### 2.3 Strains, media and cultivation techniques

*Geobacter sulfurreducens* (DSM 12127, active culture obtained from the Deutsche Stammsammlung von Mikroorganismen und Zellkulturen GmbH, Braunschweig, Germany) was cultivated in DSM 826 medium, which was made as described by the DSMZ. The strain was cultivated under 80:20 ($N_2$:$CO_2$) gas atmosphere at a temperature of 30 °C. Cells were subcultured every seven days in 200 mL septum flasks to a concentration of 1 % (v/v) containing 50 mL fresh anaerobic DSM 826 medium.

### 2.4 Setup and cultivation of the microbial fuel cells

The reactor contained a gas diffusion cathode (mixed manganese oxide on a PTFE layer contacted with a nickel net (82011, Gaskatel GmbH, Kassel, Germany) and a carbon fabric anode (ACC-5092-15, Kynol, Hamburg, Germany) were assembled and contacted with graphite foil as described before. The carbon fabric anode was desorbed at 100 °C for 24 h, wetted in isopropanol for 1 h and washed three times with double-distilled $H_2O$ prior use. After assembling the reactor, 225 mL of autoclaved DSM 826 medium was purged with a 80:20 ($N_2$:$CO_2$) gas mixture (Aligal 12, Air Liquide, Paris, France) at a flow of 30 mL $min^{-1}$ to ensure anoxic conditions in a feed vessel for 1 h. Then the reactor (V = 90 mL) was filled with a peristaltic pump and the retention time was set to 1.7 h and the medium was recirculated back into the feed vessel to ensure anaerobic conditions.

*G. sulfurreducens* cells in stationary phase (after 3 to 7 d) were washed in an equal volume of DSM 826 medium omitting fumarate as a soluble electron acceptor and the feed vessel of the MFC was inoculated with 10 % (v/v) of the culture. The vessel was purged with a 80:20 ($N_2$:$CO_2$) gas mixture (Aligal 12, Air Liquide, Paris, France) at a flow of 30 mL $min^{-1}$ to maintain anoxic conditions. Medium was pumped with a retention time of 1.7 h in loop-mode and recirculated through the MFCs for 76 h, afterwards it was switched to continuous mode with the same retention time and fresh DSM 826 medium containing 0.5 g $L^{-1}$ acetate was fed continuously in the MFC. The external circuit was closed and a 1 kΩ resistance was used as a load. The potential drop was measured using a Keithley 2000 Multimeter (Keithley Instruments, Cleveland, OH, USA) and current was then determined using Ohm's law.

### 2.5 Analysis of biofilm distribution using fluorescence microscopy

After approximately 14 d of cultivation, the MFCs were opened up and 1 cm x 1 cm samples at different locations (top: left, middle and right; middle: left, middle and right; bottom: left, middle and right) of the anode were taken to investigate the biofilm distribution. Biofilm organisms were stained by DNA binding 4',6-diamidino-2-phenylindole (DAPI). Samples were incubated for 1 min in 1 µg $mL^{-1}$ DAPI in

phosphate-buffered saline protected from light (PBS; 8 g $L^{-1}$ NaCl, 0.2 g $L^{-1}$ KCl, 1.42 g $L^{-1}$ $Na_2HPO_4$, 0.27 g $L^{-1}$ $KH_2PO_4$). After incubation the samples were washed in PBS for 1 min and pictures were taken using a Axio Imager Z1m fluorescence microscope equipped with a HBO 100 laser, transmission light HAL 100 and a DAPI filter (Zeiss, Oberkochen, Germany). Excitation/emission wavelengths were set to 358/461 nm. Pictures were taken and analyzed using the software Axiovision Rel. 4.6. (Zeiss, Oberkochen, Germany).

### 2.6 Analytics

Acetate was measured by HPLC (Prominence 20 series, Shimadzu Deutschland GmbH, Duisburg, Germany) equipped with a Rezex ROA-Organic Acid 8% H+ 300x7.8 mm (Phenomenex, Aschaffenburg, Germany) column via a photo diode array detector (SPD-M20A, Shimadzu Deutschland GmbH, Duisburg, Germany) at the detection wavelength of 209 nm. Sulfuric acid (5 mM) was used as mobile phase with a flow of 0.6 mL $min^{-1}$ at 60 °C over a total run time of 30 min. Quantification was done using a calibration curve with an external standard in the range of 0 to 20 mM acetate. Coulombic efficiency (CE) is calculated from the ratio of total recovered charge by integrating the current over time to the theoretical charge that can be produced from acetate. Theoretical charge is calculated from $Q_{th} = n\ z\ F$, where n is the amount of acetate in mol, $z$ the amount of electrons released by oxidation (in the case of acetate $z = 2$) and $F$ is the Faraday constant, which is 96485 C $mol^{-1}$, resulting in equation 6:

$$\mathrm{CE} = \frac{\int_0^t I\,dt}{n\,z\,F} \qquad (6)$$

## 3 Results and Discussion

### 3.1 Influence of perpendicular flow through a carbon fabric anode on the current of a flat-plate microbial fuel cell

Experiments with a *Geobacter sulfurreducens* based MFC were done in the developed reactors to investigate, how the flow setups (parallel *vs.* perpendicular flow through the anode) affect current and

power generation in the flat-plate reactor. Perpendicular flow through the porous anode in batch experiments shortened the lag-time in current production compared to a parallel flow from approximately 12 h to 4 h, respectively (Figure S2). The results were repeatable and indicate that the lag-time is related to nutrient deficiencies, which are reduced by changing the flow setup. Maximum currents were 0.55 mA and 0.45 mA for perpendicular flow through the porous anode vs. parallel flow, respectively, in the batch mode. After 76 h of start-up in batch-mode the MFCs were switched to continuous mode for the following experiments. In continuous mode the maximum currents were reached after 12 d for perpendicular flow through the porous anode vs. 7 d for parallel flow and were 0.52 mA and 0.29 mA (45.1 mW $m^{-2}$ and 14 $mWm^{-2}$ using an external resistance of 1 kΩ), respectively (Figure 2). Interestingly, the acetate consumption is comparable for both flow setups and the current efficiency is less for the parallel flow vs. the perpendicular flow. Therefore, the higher current production for perpendicular flow can be explained by an increased current efficiency. More acetate is converted by releasing the excess electrons to the anode rather than oxygen. Oxygen diffuses across the cathode as convective transport into the bulk of the MFC and is then transported in parallel to the anode to the outlet. This can be explained by the altered flow setup: oxygen, which is introduced by the air-breathing cathode, is kept away from the biofilm due to the perpendicular flow. In this study a current increase by a factor of 1.8 and a power density increase by a factor of 3.2 were measured using a porous carbon fabric anode with an external resistance of 1 kΩ. Cheng *et al*. have reported a power density increase of approx. 1.1 fold using a plain carbon cloth electrode in a continuous cubic reactor setup with an external resistance of 1 kΩ [13]. Differences to this study can most likely be explained by the differences in the used geometries and biological variations.

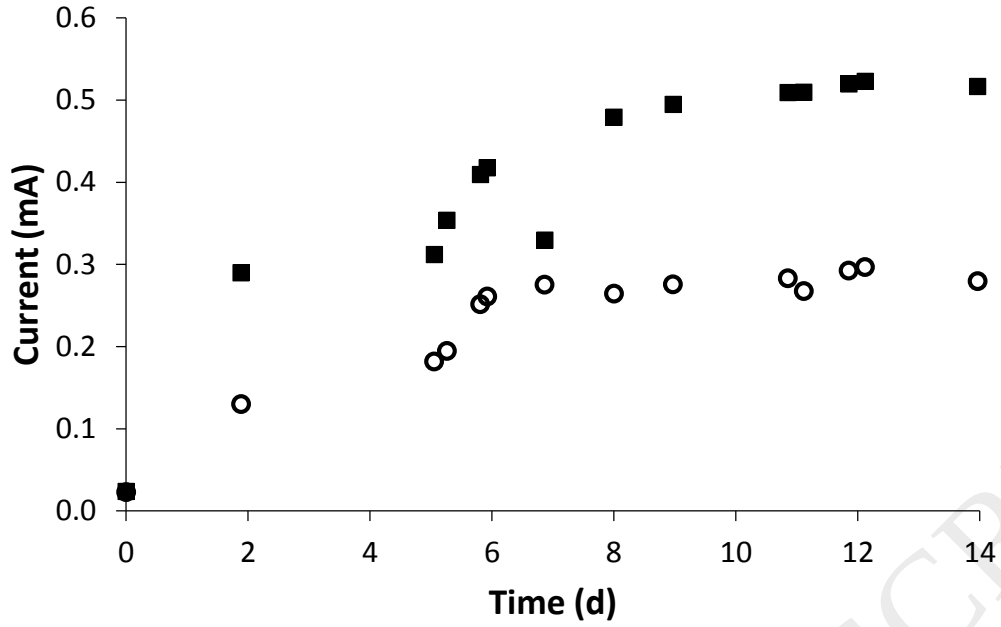


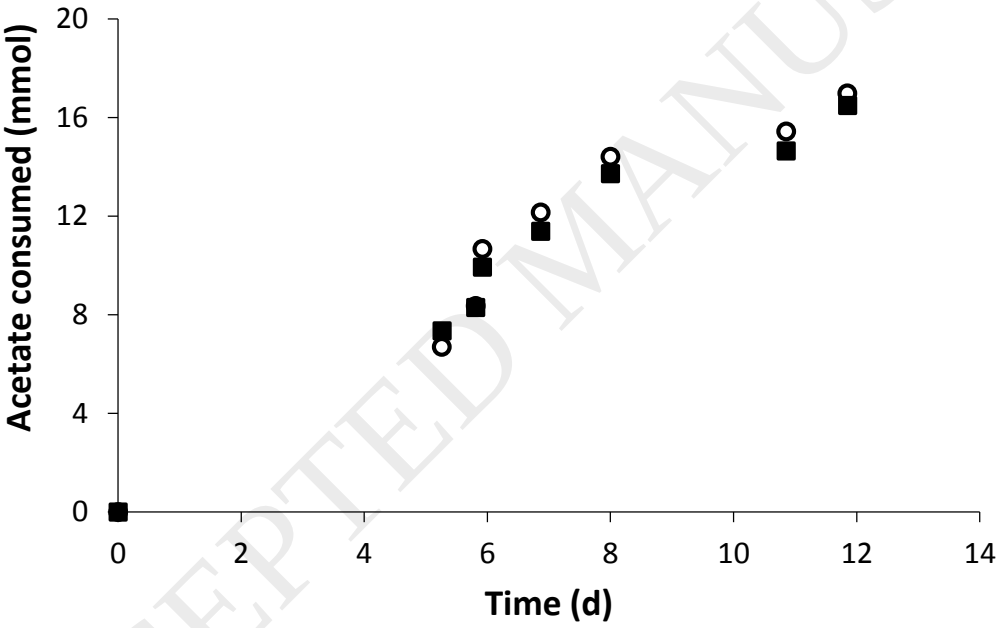


**Figure 2: Current output and consumed acetate of a flat-plate MFC with an electrode spacing of 1 cm comparing the perpendicular flow through a porous anode (squares) *vs.* parallel flow (circles) in a continuous flow mode (start-up in loop mode is shown in Figure S2) with 0.5 g $L^{-1}$ acetate as carbon source with a retention time of 1.7 h in n=2.**

Acetate consumption is comparable between the two reactors and the corresponding inlet setups and consumed 16.5 and 17 mmol acetate after 14 d, respectively. It can be assumed, that the metabolic activity was not affected by the flow regime in the MFC. Current efficiencies were 3.7 % for the

perpendicular flow setup and 2 % for parallel flow, respectively. This is an increase for the perpendicular flow through the porous anode by a factor of 1.9 and may explain the higher current production for this setup. Typical values of current efficiencies are in the range of 10 to 40 % in literature compared to the much lower values obtained in this work, which can be explained by the operation in an aerobic lab environment [13].

### 3.2 Comparison of biofilm distribution on electrodes for both inlet applications with the measured biofilm distribution on the anode

Biofilm distribution of the two inlet setups was analyzed and compared after continuous cultivation of 14 days on different parts of the carbon fabric anode. DNA of the biofilm was stained with DAPI and analyzed using a fluorescence microscope. Cells are shown in blue and the porous carbon fabric anode is black. For the perpendicular flow through the porous anode a biofilm is only detectable at the bottom part of the MFC (Figure 3). For the parallel flow in general a lower degree of biofilm is visible (Figure 3). This explains the lower current production of 0.29 mA vs. 0.52 mA for parallel flow *vs.* the perpendicular flow through the porous anode. Further pictures of the other parts of the anode can be found in the Supplementary Information (Figure S3 and Figure S4). Most likely the cells adsorb to the carbon fabric directly after entering the reactor since it is known, that the material has autosorptive properties [21].

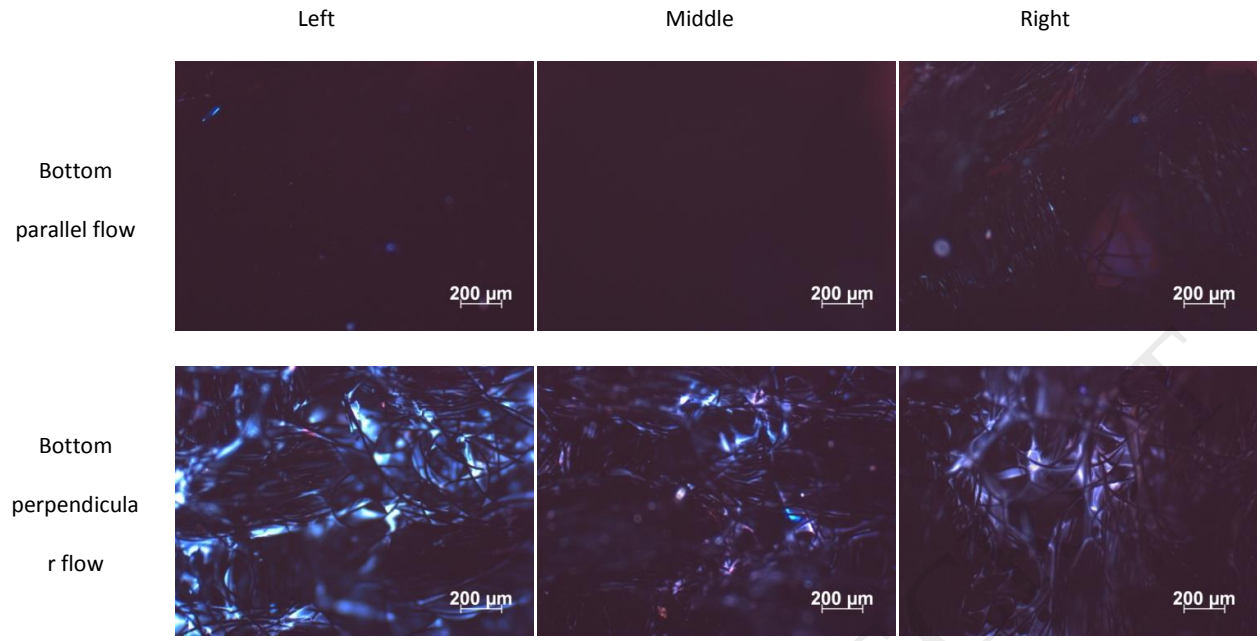


**Figure 3: Biofilm distribution of *Geobacter sulfurreducens* at different points in the microbial fuel cell after 14 days of an perpendicular flow through the porous anode visualized by DAPI staining of the cells (blue) and a fluorescence microscope. Inlet position was at the bottom right for the parallel flow and in the bottom middle for the perpendicular flow, respectively.**

### 3.3 FEM simulation of flow and concentration profiles for different MFC configurations

After observing the increased MFC performance and looking at the biofilm distribution a finite element simulation was constructed for each flow configuration in order to attempt to understand the resulting experimental performance in terms of the transport properties of each system. Besides the hindered oxygen diffusion towards the anode, also improved substrate distribution due to a better mass transport has been reported to be responsible for an increased MFC performance [13,16]. In this study, we used a carbon fabric with a porosity of 0.86 and a permeability of $10^{-10}$ $m^2$ experimentally, but also performed simulations with parametric sweeps of both, porosity and permeability, to assess the impact these parameters could have on the resulting fluid and substrate concentration profiles for each flow configuration.

Simulation results were obtained in order to investigate the influence of electrode properties on the substrate distribution, pressure drops and the ratio of advective transport rate and diffusive transport rate (Peclet number), which can have a strong influence on MFC performance. Comparing the results

of the simulations for the different inlet setups may help explaining the experimental results discussed before. Therefore, an inlet of uniform concentration into a substrate depleted system (the porous anode and the MFC) was simulated with a normalized concentration of 1 as the steady-state. Figure 4 shows the normalized concentration profile of a substrate in the porous layer *vs.* time for the two simulated flow setups. For perpendicular flow, the porous layer achieved steady-state after a time of 10 h while for a parallel flow it took close to 30 h (simulated times) for a complete distribution of the substrate in the porous layer. These differences in the simulations indicate that the effect on current output discussed in section 3.1 for the used carbon fabric electrode (ε=0.86 and $\kappa=10^{-10}$ $m^2$) is due to differences in substrate distribution for the two setups. The simulations reveal possible substrate limitations for the biofilm in certain areas of the anode for the case of parallel flow.

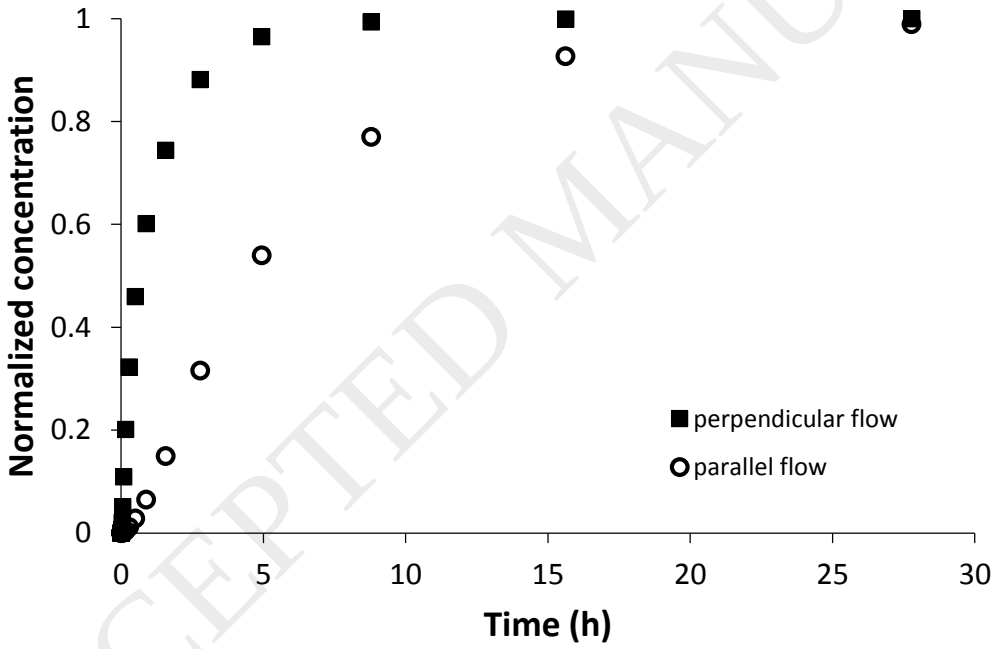


**Figure 4: Normalized concentration profiles in the porous layer (i.e. the carbon fabric anode) *vs.* time in the perpendicular flow setup (closed squares) and parallel flow to the anode (open circles).**

Looking at the estimated Peclet numbers through the porous layer, which describe the ratio of convective mass transport (fast transport by convection) and diffusive mass transport (slow transport due to molecular diffusion), support this explanation. For the perpendicular flow a Peclet number of 1.9 vs. 0.004 for parallel flow was estimated over the whole electrode based on the average velocity

and substrate diffusion coefficients, indicating a shift from diffusion-dominated transport in the parallel flow system to a slight convection-dominated regime in the perpendicular flow MFC. As illustrated in the resulting concentration vs. time plots in the porous layer, increasing the rate of convective transport is beneficial to eliminating substrate limitations (Figure 4). One can discuss however, that the advantage of this increased substrate availability is outweighed by an increased pressure drop in the system and possible clogging due to biofilm growth. However, Cheng et al. reported, that there was no blocking of the electrode over a time period of 42 days with glucose as a substrate and over 100 h for real waste water with a perpendicular inlet [13]. In this study as well, no clogging of the electrode was observed over a time period of 14 days. The simulations also showed an increase of the pressure drop from 1 mPa to 34 mPa by changing the inlet flow setup from parallel to perpendicular, respectively, however overall pump power requirements are negligible for both setups given the flow rates involved. Flow in MFCs is usually slow due to low decomposition rates of the organic loading leading to high hydraulic retention times and a laminar flow regime. The increased current output with perpendicular flow through the porous anode can then be explained by increased convective transport and a general improvement in the substrate distribution throughout the entire porous cloth in the case of perpendicular flow (Figure 5). The simulated substrate distribution does also fit to the observed biofilm on the carbon fabric anode as discussed before (Figure 3).

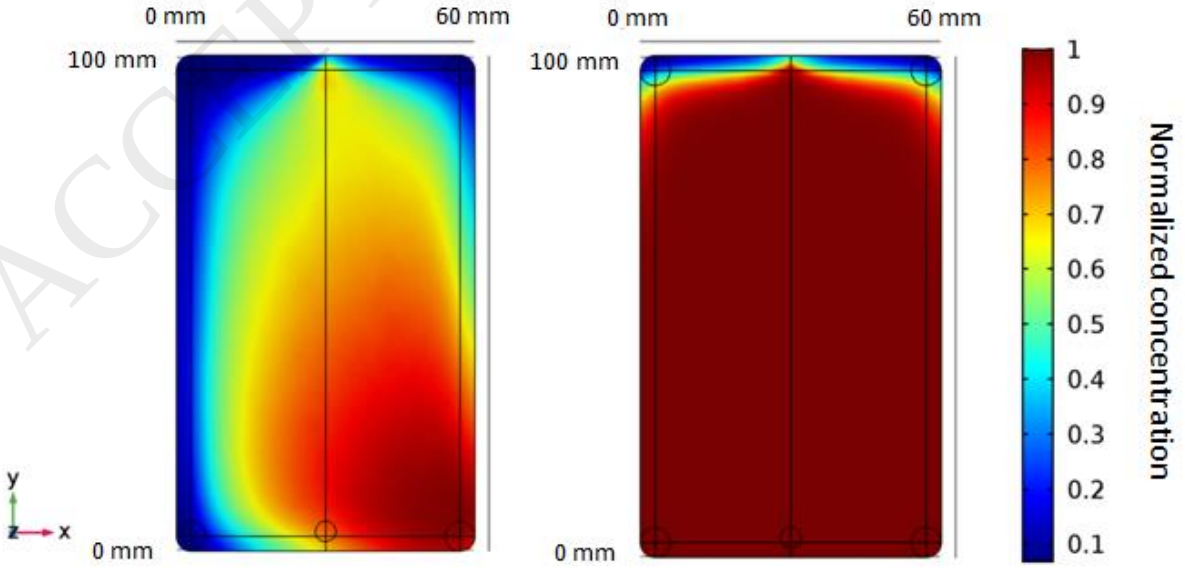

**Figure 5: Normalized concentration profiles in the porous layer (i.e. the carbon fabric anode) after 5 h in at parallel flow (left, inlet at the bottom right) and perpendicular flow through the anode (right, inlet in the middle at the bottom).**

Since the electrode properties seem to be important for the MFC performance further simulations with changes in porosity and permeability were performed to estimate what properties would be interesting to investigate in future studies. Figure S5 shows that a further increase in permeability would lead to a faster substrate distribution for the perpendicular flow setup. Varying the porosity did not lead to a significant change of the distribution. At permeabilities greater than $10^{-11}$ $m^2$ no further increase of speed of saturating the porous layer with substrate is shown in the simulations. Permeability affects the degree of flow dispersion (uniformity through the bottom). The more resistive it is the more flow will spread out to make sure it can go through the cloth. Substrate distribution is not affected by changing porosity and permeability for the parallel flow setup, this is governed by molecular diffusion from the bulk into the porous layer and will not transport through the layer before exiting and only the electrode surface area facing the medium can be accessed by the electroactive microorganisms. For perpendicular flow also deeper parts of the electrode are provided with substrate and can be accessed by the electroactive microorganisms. Therefore it can be concluded, that for the system considered, the inlet flow configuration is more important than the properties of the cloth for MFC performance.

While substrate distribution is increased for the perpendicular flow at higher permeabilities, as mentioned also an increased pressure drop is found (Figure S6). For parallel flow the pressure drop is nearly constant. This can be explained due to the fact that the inlet flow does not have to go through higher flow-resistance area of the electrode itself vs. the case of a perpendicular inlet where the flow is forced through the porous layer. Peclet numbers, which describe the ratio of convection (advection) to diffusion, are influenced by the porosity for the perpendicular flow setup (Figure S7). With decreasing porosities of the electrode from 0.8 to 0.4, the Peclet number increases in an exponential fashion from approximately 2 to 6 and convection dominates, which ensures a fast substrate transport. For the parallel inlet setup, the Peclet numbers are several orders of magnitude lower compared to

the perpendicular flow setup in all cases. Permeability and porosity influence the Peclet number, which is highest at a porosity of 0.4 and a permeability of $10^{-8}$ m2 (Figure S7). For perpendicular flow there is no significant change in the diffusive contribution compared to the convective contribution, while for parallel flow increasing porosity increases the diffusion coefficient and therefore enhances transport (as it is in a diffusion-dominated regime). Also increasing permeability makes the fluid more likely to transport through the cloth due to a lower resistance. Cheng et al. suggested using greater overall porosities to prevent clogging in real waste water treatment [13]. This would prevent clogging, however, the simulations show that an increased porosity could lead to a lower Peclet number which would possibly lead to a lowered convective transport and negate the positive effect.

An alternative for directing the flow through the anode could be the insertion of internal structures to ensure a better distribution of the substrates [8]. The anode itself also could be altered geometrically to ensure a better substrate distribution [22]. Also completely different reactor designs with serpentine flows or flat plate reactors, where the flow is directed along the anode, have been reported [23,24]. However, these strategies have the disadvantage of increased investment costs and complexity of design. Despite their promising performances in larger scales, these reactor concepts may not suitable for a scale-up due to high investment costs [23].

## 4 Conclusion and Outlook

This study combines experiments for single-chamber flat-plate MFCs and simulations of the substrate distribution in porous electrode materials to identify mass-transport related limitations. Experimental results showed an increased current output by altering the inlet flow setups from a parallel to the anode flow pattern to a perpendicular flow setup. Perpendicular flow through a porous carbon electrode increased the power density by 3.2 fold *vs.* a parallel flow in the used reactor system. Simulations indicate that the increased performance of the MFC can be explained by an optimized substrate distribution if there is a perpendicular flow through the porous electrode because of an enhanced transport of substrate due to the velocity through the porous layer, while in the case of the

parallel flow system there is only a diffusional flux. The substrate is completely distributed in the porous electrode, where the biofilm is present after 10 h *vs.* 30 h for the perpendicular flow setup *vs.* the parallel inlet setup. No electrode fouling was observed for the perpendicular flow and pressure drops were comparable to the parallel inlet setup. The simulations reveal that permeability and porosity are important parameters. If the cloth is too permeable the benefits of the perpendicular inflow are reduced, because it is not distributed well and just goes through the cloth as a jet at the inlet. Therefore, permeability and also porosity should be characterized and investigated while new MFCs are built and electrodes are engineered.

## Conflict of interest

The authors declare that there is no conflict of interest.

## Acknowledgements

The authors want to thank the BMBF for funding of the work (grant no. 031A226).

## References

[1] T. Krieg, F. Enzmann, D. Sell, J. Schrader, D. Holtmann, Simulation of the current generation of a microbial fuel cell in a laboratory wastewater treatment plant, Appl. Energy. 195 (2017) 942–949. doi:10.1016/j.apenergy.2017.03.101.

[2] K. Rabaey, W. Verstraete, Microbial fuel cells: novel biotechnology for energy generation., Trends Biotechnol. 23 (2005) 291–8. doi:10.1016/j.tibtech.2005.04.008.

[3] A. Sydow, T. Krieg, F. Mayer, J. Schrader, D. Holtmann, Electroactive bacteria - molecular mechanisms and genetic tools, Appl. Microbiol. Biotechnol. 98 (2014) 8481–8495. doi:10.1007/s00253-014-6005-z.

[4] B.E. Logan, Exoelectrogenic bacteria that power microbial fuel cells., Nat. Rev. Microbiol. 7 (2009) 375–381.

[5] T. Krieg, A. Sydow, U. Schröder, J. Schrader, D. Holtmann, Reactor concepts for bioelectrochemical syntheses and energy conversion, Trends Biotechnol. 32 (2014) 645–655. doi:10.1016/j.tibtech.2014.10.004.

[6] A. Janicek, Y. Fan, H. Liu, Design of microbial fuel cells for practical application: a review and analysis of scale-up studies, Biofuels. 502 (2014) 79–92.

[7] B.E. Logan, Scaling up microbial fuel cells and other bioelectrochemical systems, Appl. Microbiol. Biotechnol. 85 (2009) 1665–1671. doi:10.1007/s00253-009-2378-9.

[8] J. Kim, H. Kim, B. Kim, J. Yu, Computational fluid dynamics analysis in microbial fuel cells with different anode configurations, Water Sci. Technol. 69 (2014).

[9] L. Zhao, J. Li, F. Battaglia, Z. He, Investigation of multiphysics in tubular microbial fuel cells by coupled computational fluid dynamics with multi-order Butler–Volmer reactions, Chem. Eng. J. 296 (2016) 377–385. doi:10.1016/j.cej.2016.03.110.

[10] J.R. Kim, H.C. Boghani, N. Amini, K.F. Aguey-Zinsou, I. Michie, R.M. Dinsdale, A.J. Guwy, Z.X. Guo, G.C. Premier, Porous anodes with helical flow pathways in bioelectrochemical systems: The effects of fluid dynamics and operating regimes, J. Power Sources. 213 (2012) 382–390. doi:10.1016/j.jpowsour.2012.03.040.

[11] A. Escapa, M.I. San-Martín, R. Mateos, A. Morán, Scaling-up of membraneless microbial electrolysis cells (MECs) for domestic wastewater treatment: Bottlenecks and limitations, Bioresour. Technol. 180 (2015) 72–78. doi:10.1016/j.biortech.2014.12.096.

[12] I. Ieropoulos, J. Winfield, J. Greenman, Effects of flow-rate, inoculum and time on the internal resistance of microbial fuel cells, Bioresour. Technol. 101 (2010) 3520–3525. doi:10.1016/j.biortech.2009.12.108.

[13] S. Cheng, H. Liu, B.E. Logan, Increased power generation in a continuous flow MFC with advective flow through the porous anode and reduced electrode spacing, Environ. Sci.

Technol. 40 (2006) 2426–2432. doi:10.1021/es051652w.

[14] E. Kipf, J. Koch, B. Geiger, J. Erben, K. Richter, J. Gescher, R. Zengerle, S. Kerzenmacher, Systematic screening of carbon-based anode materials for microbial fuel cells with Shewanella oneidensis MR-1, Bioresour. Technol. 146 (2013) 386–392. doi:10.1016/j.biortech.2013.07.076.

[15] T.H.J.A. Sleutels, R. Lodder, H.V.M. Hamelers, C.J.N. Buisman, Improved performance of porous bio-anodes in microbial electrolysis cells by enhancing mass and charge transport, Int. J. Hydrogen Energy. 34 (2009) 9655–9661. doi:10.1016/j.ijhydene.2009.09.089.

[16] T.H.J.A. Sleutels, H.V.M. Hamelers, C.J.N. Buisman, Effect of mass and charge transport speed and direction in porous anodes on microbial electrolysis cell performance, Bioresour. Technol. 102 (2011) 399–403. doi:10.1016/j.biortech.2010.06.018.

[17] D.W. Chung, M. Ebner, D.R. Ely, V. Wood, R. Edwin García, Validity of the Bruggeman relation for porous electrodes, Model. Simul. Mater. Sci. Eng. 21 (2013). doi:10.1088/0965-0393/21/7/074009.

[18] B. Tjaden, S.J. Cooper, D.J. Brett, D. Kramer, P.R. Shearing, On the origin and application of the Bruggeman correlation for analysing transport phenomena in electrochemical systems, Curr. Opin. Chem. Eng. 12 (2016) 44–51. doi:10.1016/j.coche.2016.02.006.

[19] D.A. Nield, The boundary correction for the Rayleigh-Darcy problem: Limitations of the Brinkman equation, J. Fluid Mech. 128 (1983) 37–46. doi:10.1017/S0022112083000361.

[20] P. Vanysek, Ionic conductivity and diffusion at infinite dilution, CRC Handb. Chem. Phys. 83 (2000).

[21] F. Mayer, M. Stöckl, T. Krieg, K.-M. Mangold, D. Holtmann, Adsorption of *Shewanella oneidensis* MR-1 to the electrode material Activated Carbon Fabric, J. Chem. Technol. Biotechnol. (2018). doi:10.1002/jctb.5658.

[22] S. Chen, G. He, Q. Liu, F. Harnisch, Y. Zhou, Y. Chen, M. Hanif, S. Wang, X. Peng, H. Hou, U. Schröder, Layered corrugated electrode macrostructures boost microbial bioelectrocatalysis, Energy Environ. Sci. 5 (2012) 9769. doi:10.1039/c2ee23344d.

[23] L. Zhuang, Y. Yuan, Y. Wang, S. Zhou, Long-term evaluation of a 10-liter serpentine-type microbial fuel cell stack treating brewery wastewater, Bioresour. Technol. 123 (2012) 406–412. doi:10.1016/j.biortech.2012.07.038.

[24] Y. Feng, W. He, J. Liu, X. Wang, Y. Qu, N. Ren, A horizontal plug flow and stackable pilot microbial fuel cell for municipal wastewater treatment, Bioresour. Technol. 156 (2014) 132–138. doi:10.1016/j.biortech.2013.12.104.